Proceedings of the Canadian Society for Mechanical Engineering International Congress
32nd Annual Conference of the Computational Fluid Dynamics Society of Canada
Canadian Society of Rheology Symposium
CSME/CFDSC/CSR 2025
May 25–28, 2025, Montréal, Québec, Canada

NUMBER

A MULTIBODY DYNAMICS APPROACH TO THE UNDERSTEER BUDGET

Bruce P. Minaker[1*], Tom Zhe Ma [1]

[1]Mechanical, Automotive, & Materials Engineering, University of Windsor, Windsor ON, Canada
[*]bminaker@uwindsor.ca

February 12, 2025

***Abstract*—**The well known yaw-plane (or bicycle) model has been used for many years to study the fundamentals of vehicle handling behaviour. The model captures the basic dynamics well, but makes many simplifying assumptions about the vehicle in order to allow the development of a linear set of equations.

In the late 1960's, Bundorf expanded the bicycle model to include several additional effects that are known through practical experience to influence vehicle handling, and proposed a process that has come to be known as the *understeer budget*. The process is still used today to help design vehicles for better handling performance.

Today, most vehicle handling predictions are conducted using a multibody dynamics approach, including highly sophisticated computer simulations, technology that was unavailable at the time the understeer budget was introduced.

This paper aims to reexamine the concept of the understeer budget, while making use of modern simulations tools unavailable to Bundorf, applied to an extended linear bicycle model.

***Keywords-component*—vehicle dynamics; understeer budget; bicycle model; equations of motion; multibody dynamics**

I. INTRODUCTION

The yaw plane model, also widely known as the *bicycle model*, has been used extensively for vehicle handling studies since its introduction, and has appeared in many variations in the literature. The nickname is applied because the effect of the width of the vehicle is considered unimportant for certain aspects of the model development. When the vehicle is pictured in a view from above with the width neglected, its appearance is similar to a bicycle. The model itself has no connection to bicycle dynamics. Of course, the vehicle width influences the lateral weight transfer experienced while cornering, which in turn affects tire performance. The lateral weight transfer effect on tire behaviour and peak lateral force is a significant effect. However, in the context of the yaw plane/bicycle model, one can assume the tire is operating in a linear range of performance so the axle behaviour (i.e., the combined effect of the left and right side tires) is constant in the presence of lateral load transfer in the low/moderate handling regime (up to $\sim$0.3g of lateral acceleration).

II. MODEL DEVELOPMENT

The degrees of freedom of the yaw plane model are the lateral velocity v, and the yaw velocity r of the vehicle. The forward speed u is assumed to be under driver control and held constant, and as a result is treated as a parameter of the model rather than a variable. The motion is assumed to take place on a flat and level road, so all other motions, e.g., roll or heave, are ignored. The constant forward speed is more precisely called a *nonholonomic* constraint; this implies that despite having only two velocity degrees of freedom, three position coordinates are required to fully specify the state of the vehicle: the (x, y) location of the centre of mass, and the heading angle ψ. Despite using only two degrees of freedom, the model provides a great deal of insight into vehicle handling.

The mass m and yaw moment of inertia I_{zz} are the relevant inertial properties of the vehicle, while the distances from the centre of mass to the front and rear axles, denoted a and b respectively, provide the necessary geometric information. The *cornering stiffnesses* of the front and rear tires (lumped) are denoted c_f and c_r, respectively. The steering angle of the front tires, assumed to be the same on the left and right side, is δ_f.

The equations of motion of the yaw plane model can be found by summing lateral forces, and moments around a vertical axis. The complete model, including the kinematic differential equations, is presented in (1); for a full development, see Minaker [1].

$$\begin{Bmatrix} \dot{y} \\ \dot{\psi} \\ \dot{v} \\ \dot{r} \end{Bmatrix} = \mathbf{A} \begin{Bmatrix} y \\ \psi \\ v \\ r \end{Bmatrix} + \mathbf{B}\{\delta_\mathrm{f}\} \tag{1}$$

where:

$$\mathbf{A} = \begin{bmatrix} 0 & u & -1 & 0 \\ 0 & 0 & 0 & -1 \\ 0 & 0 & -(c_\mathrm{f}+c_\mathrm{r})/mu & -(ac_\mathrm{f}-bc_\mathrm{r})/mu - u \\ 0 & 0 & -(ac_\mathrm{f}-bc_\mathrm{r})/I_{zz}u & -(a^2c_\mathrm{f}+b^2c_\mathrm{r})/I_{zz}u \end{bmatrix} \tag{2}$$

and:

$$\mathbf{B} = \begin{bmatrix} 0 \\ 0 \\ c_\mathrm{f}/m \\ ac_\mathrm{f}/I_{zz} \end{bmatrix} \tag{3}$$

In the first order form as presented, the eigenvalues of the $\mathbf{A}$ matrix will contain a repeated zero root, which happens to be related to the lateral position and heading angle states. The other two eigenvalues are typically (but not necessarily) negative or have negative real parts, indicating that if the steering angle is held constant, the yaw rate and lateral speed will both approach steady values as well. In the steady state, where $\dot{v} = \dot{r} = 0$, an algebraic relationship between the steer input and the yaw rate can be found, and is given in (4). The *yaw rate gain* r/δ_f is used as an indicator of handling ability, and varies significantly as a function of both forward speed and vehicle parameters.

$$\frac{r}{\delta_\mathrm{f}} = \frac{u}{a+b-\frac{mu^2(ac_\mathrm{f}-bc_\mathrm{r})}{(a+b)c_\mathrm{f}c_\mathrm{r}}} \tag{4}$$

The yaw rate gain will show two distinct regions of behaviour, termed *understeer*, and *oversteer*, with the term *neutral steer* used to define the border between the two regions. While precise mathematical definitions are available, in general terms, an oversteering vehicle tends to have progressively increasing yaw rate gain with speed, until the vehicle reaches a point of instability. An understeering vehicle, which is the more common and generally preferred behaviour, has increasing yaw rate gain to a speed where the value is maximized, above which it shows a gentle asymptotic decay toward a fixed limit value. The neutral steer behaviour has linear increase in yaw rate gain with speed. An example is shown in Fig. 1.

The understeer behaviour can be quantified using the *characteristic speed* u_char, the speed where the yaw rate gain is maximized. To find the characteristic speed:

$$\frac{d}{du}\left(\frac{r}{\delta_\mathrm{f}}\right) = \frac{d}{du}\left(\frac{u}{a+b-\frac{mu^2(ac_\mathrm{f}-bc_\mathrm{r})}{(a+b)c_\mathrm{f}c_\mathrm{r}}}\right) = 0 \tag{5}$$

Taking the derivative of this fraction, and recognizing that only the numerator of the result need be equated to zero gives:

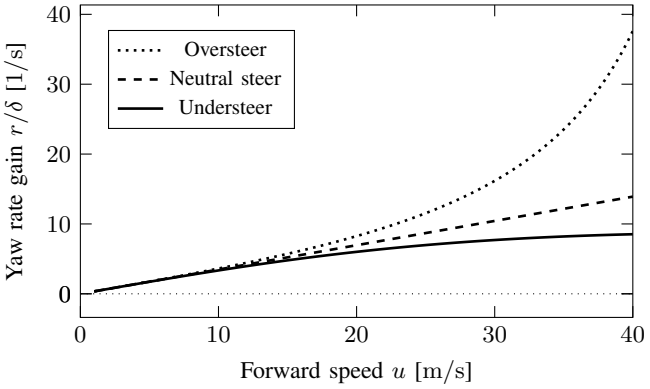

Figure. 1. Yaw rate gain, showing the distinct behaviour of oversteer and understeer configurations, and the neutral steer transition

$$\left(a+b-\frac{mu^2(ac_\mathrm{f}-bc_\mathrm{r})}{(a+b)c_\mathrm{f}c_\mathrm{r}}\right) - u\left(-\frac{2mu(ac_\mathrm{f}-bc_\mathrm{r})}{(a+b)c_\mathrm{f}c_\mathrm{r}}\right) = 0 \tag{6}$$

or:

$$u = u_\mathrm{char} = \sqrt{\frac{(a+b)^2c_\mathrm{f}c_\mathrm{r}}{m(bc_\mathrm{r}-ac_\mathrm{f})}} \tag{7}$$

Note that substituting this speed back into the yaw rate gain gives:

$$\frac{r}{\delta_\mathrm{f}} = \frac{u}{a+b+a+b} = \frac{u}{2(a+b)} \tag{8}$$

In other words, the steady state yaw rate gain of an understeering vehicle at its characteristic speed is half of the yaw rate gain of a neutral steering vehicle (where $ac_\mathrm{f} = bc_\mathrm{r}$) of the same wheelbase at the same speed. (This is the SAE definition of characteristic speed. [2])

Now the *understeer angle* α_u can be defined as the difference between the rear and front tire slip angles. In the original yaw plane model, it is assumed that the tires do not change their orientation as a result of loads or vehicle state, so the slip angles are computed from the vehicle states using kinematics:

$$\alpha_\mathrm{u} = \alpha_\mathrm{r} - \alpha_\mathrm{f} \tag{9}$$

where:

$$\begin{Bmatrix} \alpha_\mathrm{f} \\ \alpha_\mathrm{r} \end{Bmatrix} = \frac{1}{u}\begin{bmatrix} 1 & a \\ 1 & -b \end{bmatrix}\begin{Bmatrix} v \\ r \end{Bmatrix} - \begin{Bmatrix} \delta_\mathrm{f} \\ 0 \end{Bmatrix} \tag{10}$$

Substituting gives:

$$\alpha_\mathrm{u} = \delta_\mathrm{f} - \frac{(a+b)r}{u} \tag{11}$$

Recognizing the term $(a+b)r$ as the lateral velocity of the front axle relative to the rear axle, one can interpret the understeer angle as the difference between the steering angle and the direction of the relative velocity vector. The steady state *understeer angle gain* is then:

$$\begin{aligned}\frac{\alpha_{\mathrm{u}}}{\delta_{\mathrm{f}}} &= 1 - \frac{(a+b)r}{u\delta_{\mathrm{f}}} \\ &= 1 - \frac{a+b}{a+b-\frac{mu^2(ac_{\mathrm{f}}-bc_{\mathrm{r}})}{(a+b)c_{\mathrm{f}}c_{\mathrm{r}}}} \\ &= \frac{mu^2(ac_{\mathrm{f}}-bc_{\mathrm{r}})}{mu^2(ac_{\mathrm{f}}-bc_{\mathrm{r}})-(a+b)c_{\mathrm{f}}c_{\mathrm{r}}}\end{aligned} \tag{12}$$

The steady state understeer angle gain of an understeering vehicle at the characteristic speed becomes:

$$\frac{\alpha_{\mathrm{u}}}{\delta_{\mathrm{f}}} = 1 - \frac{(a+b)r}{u\delta_{\mathrm{f}}} = 1 - \frac{(a+b)}{u}\frac{u}{2(a+b)} = 0.5 \tag{13}$$

This is an important result, as it provides a means of computing the *understeer gradient* k_{us}. The understeer angle gain can be computed over a range of speeds from only the yaw rate, forward speed, wheelbase, and steer angle, and used to determine the characteristic speed, which is also related to the understeer gradient, like so:

$$u_{\mathrm{char}} = \sqrt{\frac{(a+b)^2 c_{\mathrm{f}}c_{\mathrm{r}}}{m(bc_{\mathrm{r}}-ac_{\mathrm{f}})}} = \sqrt{\frac{g(a+b)}{k_{\mathrm{us}}}} \tag{14}$$

This implies:

$$k_{\mathrm{us}} = \frac{mg}{a+b}\left(\frac{b}{c_{\mathrm{f}}} - \frac{a}{c_{\mathrm{r}}}\right) = \frac{Z_{\mathrm{f}}}{c_{\mathrm{f}}} - \frac{Z_{\mathrm{r}}}{c_{\mathrm{r}}} \tag{15}$$

where Z_{f} and Z_{r} are the weight loads on the front and rear axle, respectively. If the cornering radius R is defined as $R = u/r$, this also implies:

$$\delta_{\mathrm{f}} = \frac{a+b}{R} + k_{\mathrm{us}}\frac{u^2}{gR} = \frac{a+b}{R} + \alpha_{\mathrm{u}} \tag{16}$$

where:

$$\alpha_{\mathrm{u}} = k_{\mathrm{us}}\frac{u^2}{gR} \tag{17}$$

This expression can be interpreted as meaning that the steady state steer angle consists of two components: the first to account for the kinematics of the corner, and the second (α_{u}) to account for tire slip behaviour. The slip component is the understeer gradient, multiplied by the lateral acceleration in units of 'g' (gravities).

Now, when examining (15), one can recognize that the presence of the c_{f} and c_{r} terms in the denominator represent a kind of flexibility, i.e., the amount of tire slip angle per unit lateral load. One can consider that the weight terms Z_{f} and Z_{r} in this case represent not only a vertical load, but equivalently the amount of lateral load the axle must carry per 'g' of lateral acceleration, (i.e., lateral acceleration measured in units of gravities). So the term $Z_{\mathrm{f}}/c_{\mathrm{f}}$ can be interpreted as the amount of slip angle at the front axle per unit of lateral acceleration. The understeer gradient is the difference between the slip per unit acceleration of the two axles.

This insight was discussed by Bundorf in his landmark 1968 paper 'The Influence of Vehicle Design Parameters on Characteristic Speed and Understeer' [3]. In this paper, Bundorf expands on this idea of slip per unit acceleration to provide an enhanced understeer gradient that includes several additional effects, namely, suspension flexibility (the tires steer relative to the chassis in response to external load), roll steer (the tires steer as a result of suspension kinematics as the vehicle rolls), camber change (the tire cambers under load and with roll, which affects tire force), and lastly, pneumatic trail. (As a consequence of the deflected shape of the tire contact patch, the lateral tire force acts slightly behind the centre of the tire by a small distance called the pneumatic trail.) Because the pneumatic trail is small compared to the wheelbase, its effect on vehicle motion is small when suspension flexibility is neglected. However, it plays a significant role in determining the amount of wheel steer when suspension flexibility is considered. Pneumatic trail effects are included through the addition of aligning moment stiffness terms that help to characterize the tire. Bundorf's updated expression is reproduced in (18), using his original notation.

$$\begin{aligned}K_{\mathrm{us}} = &\frac{W_{\mathrm{f}}}{2C_{\alpha\mathrm{f}}}(1+E_{\mathrm{af}}N_{\alpha\mathrm{f}})\left(1+\frac{N_{\alpha\mathrm{r}}}{bC_{\alpha\mathrm{r}}}\right) \\ &- \frac{W_{\mathrm{r}}}{2C_{\alpha\mathrm{r}}}(1-E_{\mathrm{ar}}N_{\alpha\mathrm{r}})\left(1-\frac{N_{\alpha\mathrm{f}}}{aC_{\alpha\mathrm{f}}}\right) \\ &+ E_{\mathrm{ff}}\frac{W_{\mathrm{sf}}}{2} + E_{\mathrm{fr}}\frac{W_{\mathrm{sr}}}{2} + K'_{\phi}\left(E_{\mathrm{sf}}+E_{\mathrm{sr}}\right) \\ &+ K'_{\phi}\left((1+E_{\mathrm{af}}N_{\alpha\mathrm{f}})\frac{C_{\gamma\mathrm{f}}\Gamma_{\mathrm{f}}}{C_{\alpha\mathrm{f}}} + (1-E_{\mathrm{ar}}N_{\alpha\mathrm{r}})\frac{C_{\gamma\mathrm{r}}(-\Gamma_{\mathrm{r}})}{C_{\alpha\mathrm{r}}}\right)\end{aligned} \tag{18}$$

The notation is explained in Table I. Note that Bundorf's definition of the tire cornering stiffness, e.g., $C_{\alpha\mathrm{f}}$ is the value for a single tire, where the value used in the development of the model above (c_{f}) used a lumped value representing the sum of the left and right side tires. Thus, the appearance of the factor of two in some places in his expression. Further, he makes the distinction between axle weight (the total weight carried by the tires of a particular axle) and sprung axle weight (the weight carried by the springs of a particular axle, i.e., the total weight, less the weight of the suspension components).

An examination of (18) shows that the updated understeer gradient calculcation involves the summation of several terms, each representing a particular effect. The act of summing of the many contributions to understeer or oversteer behaviour has come to be known as the *understeer budget*. It allow vehicle manufacturers to adjust or correct overall handling behavior by choosing vehicle design parameters that affect particular terms in the understeer budget. Bundorf and Leffert expand on this concept in a following paper [4].

It is noteworthy that in the development of the second term in the above list, the Bundorf model does make one approximation: that the addition of pneumatic trail has a negligible effect on the wheelbase. Because the pneumatic trail is very small and very similar at the front and rear, this is very reasonable approximation.

TABLE. I
VEHICLE PARAMETERS FOR BUNDORF MODEL

Notation	Definition
W_{f}	front axle weight force [N]
W_{r}	rear axle weight force [N]
W_{sf}	front axle sprung weight force [N]
W_{sr}	rear axle sprung weight force [N]
$C_{\alpha\mathrm{f}}$	front cornering stiffness (per tire) [N/rad]
$C_{\alpha\mathrm{r}}$	rear cornering stiffness (per tire) [N/rad]
$N_{\alpha\mathrm{f}}$	front aligning moment stiffness (per tire) [Nm/rad]
$N_{\alpha\mathrm{r}}$	rear aligning moment stiffness (per tire) [Nm/rad]
E_{ff}	front deflection steer lateral force coefficient [rad/N]
E_{fr}	rear deflection steer lateral force coefficient [rad/N]
E_{af}	front deflection steer aligning torque coefficient [rad/Nm]
E_{ar}	rear deflection steer aligning torque coefficient [rad/Nm]
K'_{ϕ}	total roll flexibility [rad/g]
E_{sf}	front roll steer coefficient []
E_{sr}	rear roll steer coefficient []
Γ_{f}	front roll camber coefficient []
Γ_{r}	rear roll camber coefficient []
$C_{\gamma\mathrm{f}}$	front camber stiffness (per tire) [N/rad]
$C_{\gamma\mathrm{r}}$	rear camber stiffness (per tire) [N/rad]

III. MULTIBODY DYNAMICS

The results in this paper are generated by a multibody dynamics vehicle motion simulation, using the equations of motion generator code EoM, developed by the University of Windsor Vehicle Dynamics and Control research group [5]. The EoM software is able to generate equations of motion for complex three dimensional multibody systems, but restricts the result to linear equations. It is freely available on the code sharing website www.github.com.

The EoM code generates the equations in *descriptor state space* form, before converting them to the standard state space form shown in (19). This process allows the inclusion of any differential algebraic equations (DAEs) that may result from systems that contain massless bodies.

$$\begin{Bmatrix} \dot{\boldsymbol{x}} \\ \boldsymbol{y} \end{Bmatrix} = \begin{bmatrix} \mathbf{A} & \mathbf{B} \\ \mathbf{C} & \mathbf{D} \end{bmatrix} \begin{Bmatrix} \boldsymbol{x} \\ \boldsymbol{u} \end{Bmatrix} \tag{19}$$

The vectors $\boldsymbol{x}$, $\boldsymbol{y}$, and $\boldsymbol{u}$ represent the states of the system, the outputs, and the inputs, respectively. The state vector may be the translational and rotational displacements and velocities, but there are other possibilities. The $\mathbf{A}$, $\mathbf{B}$, $\mathbf{C}$, and $\mathbf{D}$ matrices are the system, input, output, and feed-through, respectively.

By identifying the yaw rate as an element in the output vector, and the steer angle as an input, the EoM software can easily compute the raw rate gain and understeer angle gain for a variety of vehicle models and configurations. Computing the understeer angle gain over a range speeds allows one to determine the characteristic speed, and from there, the understeer gradient.

IV. ENHANCED MULTIBODY VEHICLE MODELS

Several multibody vehicle models were developed to compare against the Bundorf equation:

- Model 1: the traditional single body yaw plane model, but with pneumatic trail added
- Model 2: a three body yaw plane model, with flex steer and pneumatic trail
- Model 3: a three body yaw plane model, with roll steer and pneumatic trail
- Model 4: a five body yaw plane model, with roll steer, flex steer, and pneumatic trail
- Model 5: a five body yaw plane model, with roll steer, flex steer, camber effects, and pneumatic trail

An example vehicle is used to compare the results of the various multibody models to Bundorf's model. Note that the mass of the example vehicle is $m = 1914$ kg, and the dimensions of the wheelbase are $a = 1.473$ m and $b = 1.403$ m. The values of the other parameters are given in Table II. Note that the values are given using the sign convention used by Bundorf, where any positive coefficient will contribute to understeer, any negative coefficient will contribute to oversteer, with the exception of Γ_{r}, which is reversed. (Some analysts use other sign conventions.)

TABLE. II
VEHICLE PARAMETERS FOR EXAMPLE MODEL

Notation	Definition	Notation	Definition
$C_{\alpha\mathrm{f}}$	82334 [N/rad] (per tire)	W_{f}	9159.7[N]
$C_{\alpha\mathrm{r}}$	86345 [N/rad] (per tire)	W_{r}	9616.7 [N]
$N_{\alpha\mathrm{f}}$	1948 [Nm/rad] (per tire)	W_{sf}	8243.7 [N]
$N_{\alpha\mathrm{r}}$	2177 [Nm/rad] (per tire)	W_{sr}	8655.0 [N]
E_{ff}	1.0123e-6 [rad/N]	E_{sf}	0.11 []
E_{fr}	1.8151e-7 [rad/N]	E_{sr}	0.03 []
E_{af}	4.1015e-5 [rad/Nm]	Γ_{f}	0.32 []
E_{ar}	-8.7441e-6 [rad/Nm]	Γ_{r}	0.26 []
K'_{ϕ}	0.0048215 [rad·s^2/m]		
$C_{\gamma\mathrm{f}}$	6532 [N/rad] (per tire)		
$C_{\gamma\mathrm{r}}$	6990 [N/rad] (per tire)		

One of the shortcomings of using the understeer angle gain approach to compute the understeer gradient is that the approach only works for understeering vehicles. With these parameters, the traditional single body yaw plane model, with no additional effects considered, predicts an oversteer behavior, i.e., there is no characteristic speed, and the understeer gradient becomes negative. In order to confirm the understeer gradient solution methodology works for the baseline vehicle, the values of a and b were temporarily swapped, giving:

$$\begin{aligned} K_{\mathrm{us}} &= \frac{W_{\mathrm{f}}}{2C_{\alpha\mathrm{f}}} - \frac{W_{\mathrm{r}}}{2C_{\alpha\mathrm{r}}} \\ &= 0.00536 \text{ rad/g} \\ &= 0.307 \text{ }^{\circ}\text{/g} \end{aligned} \tag{20}$$

The result generated by EoM for this model matches to three significant figures.

A. Pneumatic trail

All the enhanced multibody models developed allow that the lateral tire force acts on the tire behind the wheel centre as described by the pneumatic trail. The pneumatic trail is computed from:

$$pt_{\mathrm{f}} = \frac{N_{\alpha\mathrm{f}}}{C_{\alpha\mathrm{f}}}, \quad pt_{\mathrm{r}} = \frac{N_{\alpha\mathrm{r}}}{C_{\alpha\mathrm{r}}} \tag{21}$$

A single body model equivalent to the baseline bicycle model has been developed in EoM (Model 1), with the lateral force locations determined by including the pneumatic trail. The model should reproduce only the first term in the Bundorf model, as shown in (22). Using the Bundorf equation, ignoring flex steer, roll steer, and roll camber, and including only the pneumatic trail effects gives:

$$\begin{aligned} K_{\text{us}} &= \frac{W_{\text{f}}}{2C_{\alpha\text{f}}}\left(1+\frac{N_{\alpha\text{r}}}{bC_{\alpha\text{r}}}\right)-\frac{W_{\text{r}}}{2C_{\alpha\text{r}}}\left(1-\frac{N_{\alpha\text{f}}}{aC_{\alpha\text{f}}}\right) \\ &= 0.00183 \text{ rad/g} \\ &= 0.105 \ ^\circ\text{/g} \end{aligned} \tag{22}$$

Again, the EoM model matches the Bundorf equation to three significant figures.

B. Suspension flexibility

The additional steer angle of the front tire in response to lateral loads is quantified using two terms, E_{ff}, the response to lateral force F, and E_{af}, the response to restoring moments M around the tire vertical axis, generated by the tire. This restoring moment is a consequence of the pneumatic trail. The steer deflection θ can be written as:

$$\theta = E_{\text{ff}}F + E_{\text{af}}M \tag{23}$$

These steer deflections can be considered as a result of a rotation around a fictitious steer axis that can be located with a simple ratio, as follows. Consider an arm of length l_{f} fixed by a pivot to the vehicle chassis at one end, and supporting the tire at the other. Suppose a lateral spring of stiffness k reacts between the arm and the chassis at the wheel centre. If an applied force F is acting at the tire:

$$F = kx = kl_{\text{f}}\theta \Rightarrow \theta = \frac{1}{kl_{\text{f}}}F \Rightarrow E_{\text{ff}} = \frac{1}{kl_{\text{f}}} \tag{24}$$

If an applied moment M is acting on the arm:

$$M = kxl_{\text{f}} = kl_{\text{f}}^2\theta \Rightarrow \theta = \frac{1}{kl_{\text{f}}^2}M \Rightarrow E_{\text{af}} = \frac{1}{kl_{\text{f}}^2} \tag{25}$$

From (24) and (25), one can isolate expressions for the moment arm length and equivalent spring stiffness. The results are given in (26) and (27).

$$\frac{E_{\text{ff}}}{E_{\text{af}}} = \frac{1}{kl_{\text{f}}}\frac{kl_{\text{f}}^2}{1} = l_{\text{f}} \tag{26}$$

$$\frac{E_{\text{af}}}{E_{\text{ff}}^2} = \frac{1}{kl_{\text{f}}^2}\frac{k^2l_{\text{f}}^2}{1} = k \tag{27}$$

A multibody model that adds two bodies to represent the front and rear unsprung mass has been developed, constraining the wheel bodies with a hinge around a vertical axis, and a lateral spring. The constraint hinge locations and lateral spring stiffnesses were found as described above. Note that E_{f} and E_{a} values used in Bundorf's model are for one wheel; the corresponding EoM model scales both these flexibilities by one half, resulting in no change to the l values, and a doubling of k. It should also be noted that the resulting arm length value is generally very small, located only a few centimeters from the wheel centre, and the stiffness is very high, resulting in a very high frequency oscillation component in the solution of the equations of motion. However, this high frequency component does not affect the steady state solution required for the understeer gradient. This multibody model (Model 2) includes pneumatic trail, and should capture the two effects contained in the first term of Bundorf's model, as shown in (28).

In the development of the multibody models, another important point to consider is the distinction between sprung and unsprung mass. Bundorf recognizes in his equation that the lateral load carried by the tires includes the acceleration of both the sprung and unsprung mass, while the lateral load carried by the suspension results from only the sprung mass. As a rule of thumb, the unsprung mass will be about 10% of the mass supported by each axle. If one uses this rule to determine values of the sprung and unsprung masses, and treats the unsprung mass as if it were located exactly at the axles, it is noteworthy that the location of the centre of mass of the sprung mass will remain at the centre of mass of the assembly. If alternate values of the unsprung masses are used, one should take care to calculate the location of the centre of mass of the sprung mass, to ensure that the location of the mass centre of the assembly is unchanged.

Using the Bundorf equation, ignoring roll steer and roll camber, and including the flex steer and pneumatic trail effects gives:

$$\begin{aligned} K_{\text{us}} &= \frac{W_{\text{f}}}{2C_{\alpha\text{f}}}(1+E_{\text{af}}N_{\alpha\text{f}})\left(1+\frac{N_{\alpha\text{r}}}{bC_{\alpha\text{r}}}\right) \\ &\quad -\frac{W_{\text{r}}}{2C_{\alpha\text{r}}}(1-E_{\text{ar}}N_{\alpha\text{r}})\left(1-\frac{N_{\alpha\text{f}}}{aC_{\alpha\text{f}}}\right) \\ &\quad +E_{\text{ff}}\frac{W_{\text{sf}}}{2}+E_{\text{fr}}\frac{W_{\text{sr}}}{2} \\ &= 0.00531+0.00496 = 0.0103 \text{ rad/g} \\ &= 0.588 \ ^\circ\text{/g} \end{aligned} \tag{28}$$

The result generated by EoM matches closely but not exactly to the Bundorf prediction, at $0.5923 \ ^\circ\text{/g}$.

C. Roll steer

A multibody model that adds two bodies to represent the front and rear axles has been developed, constraining the axle bodies to the chassis with a hinge with a nearly longitudinal axis, slightly inclined vertically. In this case, the mass of the two bodies representing the axles was neglected, and the entire mass is lumped in the chassis body. The axle bodies are constrained in roll, while chassis roll is allowed, and restricted by a torsional spring between it and the ground. The stiffness of the torsional spring is computed from the roll flexibility value K'_{ϕ}. The rolling moment is caused by lifting the centre of mass a distance h_{G} above the ground plane. In order to simplify the model, this distance is chosen as $h_{\text{G}} = 1/m$. In this way, the rolling moment is numerically equal to the lateral acceleration.

The angle of the axes of the two hinges are computed from the E_{sf} and E_{sr} values. The front hinge is inclined upward

at the front by an angle of E_{sf} radians, while the rear hinge is inclined upward at the rear by an angle of E_{sr} radians. Note that the sign convention of E_{sf} and E_{sr} is important here. From inspection of Bundorf's equation, if $E_{\mathrm{sf}} = -E_{\mathrm{sr}}$, then the effect of roll steer is zero. In this case, the axes of the two hinges would be parallel, resulting in equal roll steer at both axles, and no effect on yaw motion. The longitudinal locations of the hinges are aligned with the lateral force, i.e., shifted rearward from the axle centres by the pneumatic trail; the vertical locations are at ground level.

This multibody model (Model 3) includes pneumatic trail, and should capture the two effects contained in Bundorf's model as shown in (29). Using the Bundorf equation, and ignoring suspension flexibility and camber change gives:

$$\begin{aligned} K_{\mathrm{us}} &= \frac{W_{\mathrm{f}}}{2C_{\alpha\mathrm{f}}}\left(1+\frac{N_{\alpha\mathrm{r}}}{bC_{\alpha\mathrm{r}}}\right) - \frac{W_{\mathrm{r}}}{2C_{\alpha\mathrm{r}}}\left(1-\frac{N_{\alpha\mathrm{f}}}{aC_{\alpha\mathrm{f}}}\right) \\ &\quad + K'_{\phi}\left(E_{\mathrm{sf}}+E_{\mathrm{sr}}\right) \\ &= 0.00183 + 0.00662 = 0.00845 \text{ rad/g} \\ &= 0.484 \text{ °/g} \end{aligned} \tag{29}$$

The value returned by the EoM model was 0.4856 °/g, agreeing well.

D. Suspension flexibility and roll steer

The next model was a five body model including both suspension flexibility and roll steer effects, along with pneumatic trail. The five body model included a sprung mass, and each axle was modelled as two rigid bodies. The first axle body was massless, and constrained to the sprung mass with a hinge and to the ground to constrain roll motion, to capture the roll steer effect, similar to Model 3. The second axle body represented the unsprung mass, and was hinged to the axle to capture the flex steer effect, as in Model 2. The centre of mass height is adjusted to be the inverse of the sprung mass only, to maintain the same roll stiffness. The equivalent Bundorf equation is given in (30).

$$\begin{aligned} K_{\mathrm{us}} &= \frac{W_{\mathrm{f}}}{2C_{\alpha\mathrm{f}}}(1+E_{\mathrm{af}}N_{\alpha\mathrm{f}})\left(1+\frac{N_{\alpha\mathrm{r}}}{bC_{\alpha\mathrm{r}}}\right) \\ &\quad - \frac{W_{\mathrm{r}}}{2C_{\alpha\mathrm{r}}}(1-E_{\mathrm{ar}}N_{\alpha\mathrm{r}})\left(1-\frac{N_{\alpha\mathrm{f}}}{aC_{\alpha\mathrm{f}}}\right) \\ &\quad + E_{\mathrm{ff}}\frac{W_{\mathrm{sf}}}{2} + E_{\mathrm{fr}}\frac{W_{\mathrm{sr}}}{2} + K'_{\phi}\left(E_{\mathrm{sf}}+E_{\mathrm{sr}}\right) \\ &= 0.00531 + 0.00496 + 0.00662 = 0.0169 \text{ rad/g} \\ &= 0.968 \text{ °/g} \end{aligned} \tag{30}$$

The EoM model gave a value of 1.0378 °/g.

E. Roll camber

Lastly, a five body model was used to capture all the effects in the Bundorf model. In this model, the structure of Model 4 was repeated, but the angle of inclination of the roll steer hinge was modified. The modified hinge angle allows the model to capture an additional steer angle. The lateral force generated by the extra steer angle is equivalent to the camber stiffness times the camber angle. The extra inclination of the hinge axis is the camber coefficient times the camber stiffness over the cornering stiffness. Note that the EoM model used double the camber stiffness, similar to cornering stiffness. Care with the sign convention is again key here to ensure the change is in the correct direction. The results are shown in Table III, along with all the previous models.

V. Results and discussion

The results show that the basic premise of conducting understeer budget analysis using simple multibody dynamic models is sound, but the method demonstrated is suitable only for understeering vehicles. Generally, the agreement between the Bundorf model and the EoM model was excellent, but the inclusion of flex steer did not agree as well as pneumatic trail and roll steer. The exact source of the discrepancy is unclear, as Bundorf did not provide any development of his equation in his paper. The authors did not explore any camber flexibility in this paper; some authors have extended the Bundorf model to include this effect [6]. In theory, it should be a matter of adjusting the flex steer stiffness to find an equivalent value, in much the same way that roll camber is included, through a ratio of camber stiffness and cornering stiffness, but in any case, camber flexibility is very small effect.

TABLE. III
Understeer Gradient results [°/g]

Model	EoM result	Bundorf model
Baseline	0.3069	0.307
Pneumatic trail	0.1048	0.105
Flex steer and pneumatic trail	0.5923	0.588
Roll steer and pneumatic trail	0.4856	0.484
Flex and roll steer and pneumatic trail	1.0378	0.968
All above plus roll camber	1.0956	0.984

Acknowledgment

The authors would like to thank Mr Tim Drotar for his enlightening lectures and insightful conversations regarding the topic. His practical experience in the field and his passion for sharing his knowledge has been invaluable.

References

[1] B. P. Minaker, *Fundamentals of vehicle dynamics and modelling: A textbook for engineers with illustrations and examples*. John Wiley & Sons, 2019.

[2] "Surface vehicle recommended practice," SAE Int'l, Warrendale, PA, Tech. Rep. SAE J670, January 2008.

[3] R. T. Bundorf, "The influence of vehicle design parameters on characteristic speed and understeer," *SAE Transactions*, pp. 548–560, 1968.

[4] R. T. Bundorf and R. L. Leffert, "The cornering compliance concept for description of vehicle directional control properties," *SAE transactions*, pp. 2278–2291, 1976.

[5] B. Minaker and R. Rieveley, "Automatic generation of the non-holonomic equations of motion for vehicle stability analysis," *Vehicle system dynamics*, vol. 48, no. 9, pp. 1043–1063, 2010.

[6] A. L. Nedley and W. J. Wilson, "A new laboratory facility for measuring vehicle parameters affecting understeer and brake steer," *SAE Transactions*, pp. 1612–1630, 1972.